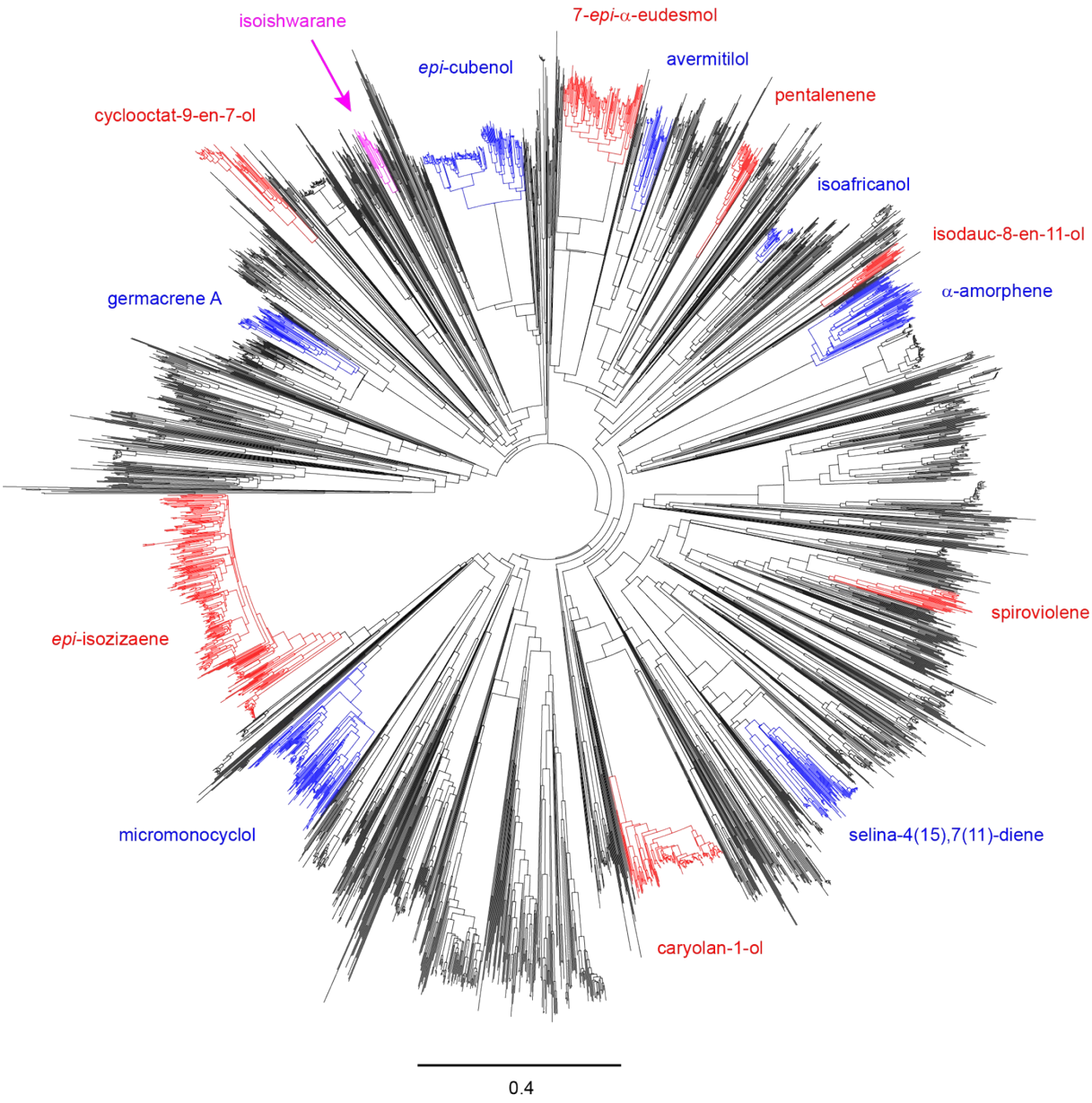

Figure S1. Phylogenetic tree constructed from 3267 amino acid sequences of bacterial terpene synthase homologs using the tree builder function of Geneious (alignment type: global alignment with free end gaps, cost matrix: Blosum45, genetic distance model: Jukes-Cantor, tree build method: neighbor-joining, gap open penalty: 8, gap extension penalty: 2). The largest branches representing functionally characterised enzymes[1-13] and their closest relatives with likely the same function are shown in blue and red. The purple arrow indicates the isoishwarane synthase from *S. lincolnensis* and its closest homologs in several other streptomycetes. The scale bar indicates the number of substitutions per site.

Strains and culture conditions

Streptomyces lincolnensis DSM 40355 was obtained from the DSMZ (Braunschweig, Germany) and was cultivated in 65 GYM (4.0 g L^{-1} glucose, 4.0 g L^{-1} yeast extract, 10.0 g L^{-1} malt extract, distilled water, pH 7.2) at 28 °C. For agar plate cultures 15.0 g agar-agar was added. *Saccharomyces cerevisiae* FY834 was cultivated in liquid YPAD medium (10.0 g yeast extract, 20.0 g peptone, 20.0 g glucose, 400 mg adenine sulphate, 1.0 L H_2O) or on SM-URA agar plates (1.7 g yeast nitrogen base, 5.0 g ammonium sulphate, 20.0 g glucose, 770 mg nutritional supplement minus uracil, 20.0 g agar-agar, 1.0 L H_2O) at 28 °C. *Escherichia coli* BL21(DE3) was grown in LB medium (10.0 g tryptone, 5.0 g yeast extract, 5.0 g NaCl, 1.0 L H_2O) at 37 °C. For agar plate cultures 16 g agar-agar was added. Kanamycin was used at a concentration of 50 µg mL^{-1}. All media were autoclaved at 121 °C for 20 min prior to use.

MLAMIPTYAEPTPPAVSPYTQRIEEHVRSLGWSLGLTETQGGQERLEAGYGRFVAWTYPEASFRDLCL
CAEWLFFTFILDDLHTLKVYDAPEAWIPVHRRLMDIINNGKDPAPPRERTPFTKALTNLSIRTRERLS
PGLRGRLNRHLDLFFQGFAEESANRFRGTPPGIDSFTHTRRLSVGMEFGFDLVELSLGVEVPKDIYET
SLFREIVEAASDVVAWQNDLHSIHLDQQRGDFHNVVIVMQHADGISLEEAIDSTVAKVQGRVADFLDA
EERLLPYLESRGVPLGTCEEILKVTAGMRQWTNGCLHWYRNTTRYAIPATPGELDQQHDHLQVLLPSL
DGASRQSCG

Figure S2. Amino acid sequence of IWS from *S. lincolnensis* (accession number WP_067429395, gene locus tag SLINC_RS09705). Highly conserved motifs are marked by yellow background.

Gene cloning and expression

The desired gene was obtained from freshly isolated genomic DNA from *S. lincolnensis* by PCR using Q5-High-Fidelity DNA polymerase (New England Biolabs, Ipswich, MA, USA) and the short primers P1_fwd and P1_rev (Table S1). PCR standard conditions were used (initial denaturation at 98 °C for 1 min, 30 cycles with denaturation at 98 °C for 15 sec, annealing at 68 °C for 30 sec and elongation at 72 °C for 30 seconds, final elongation step at 72 °C for 5 min). The obtained product was used as a template in a second PCR with the long primers P2_fwd and P2_rev to attach homology arms for homologous recombination in yeast. The elongated PCR products together with the linearised pYE-Express shuttle vector were used for a yeast homologous recombination by a standard protocol using PEG, LiOAc and salmon sperm DNA.[14,15] The transformed S*accharomyces cerevisiae* cultures were plated on SM-URA plates and grown for 3 days at 28 °C. Colonies were collected from the plates and plasmid DNA was isolated using Zymoprep Yeast Plasmid Miniprep II (Zymo Research, Irvine, USA). The isolated plasmid DNA was used for electroporation of *E. coli* BL21(DE3) electrocompentent cells. The transformed *E. coli* was grown overnight at 37 °C on LB agar plates containing kanamycin (50 µg mL^{-1}). Single colonies were selected to inoculate 6 mL LB with kanamycin. The resulting cultures were grown for 24 h to isolate plasmid DNA, yielding plasmid pYE-WP_067429395 which was checked by analytical digest and by sequencing.

Table S1. Primers used in this study.

Primer name	Nucleotide sequence (5' → 3')[a]
P1_fwd	GTGCTCGCCATGATCCCGAC
P1_rev	TCAACCGCAACTCTGCCGG
P2_fwd	GGCAGCCATATGGCTAGCATGACTGGTGGAGTGCTCGCCATGATCCCGAC
P2_rev	TCTCAGTGGTGGTGGTGGTGGTGCTCGAGTTCAACCGCAACTCTGCCGG
N126D_fwd	CACCAAGGCGCTCACG**GAT**CTGTCGATCCGTAC
N126D_rev	CGGATCGACAG**ATC**CGTGAGCGCCTTGGTG
F77I_fwd	CTTTTCTTCACC**ATT**ATCCTGGACGACCTGCAC
F77I_rev	CAGGTCGTCCAGGA**TAA**TGGTGAAGAAAAGC
T84D_fwd	CTGGACGACCTGCAC**GAT**TTGAAGGTGTATGAC
T84D_rev	CGTCATACACCTTCAA**ATC**GTGCAGGTCGTCC
L229R_fwd	GCACTCAATTCATC**GT**GACCAGCAGCGCGG
L229R_rev	CCGCGCTGCTGGTC**AC**GATGAATTGAGTGC

[a] Homology arms for homologous recombination with the linearised expression vector pYE-Express in yeast are underlined. Nucleotide exchanges in mutational primers are marked in bold.

Gene expression and enzyme purification

For gene expression a preculture of the *E. coli* transformants harbouring the plasmid pYE-WP_067429395 was grown overnight at 37 °C in LB medium containing kanamycin. The expression cultures were then inoculated using 1 mL L^{-1} of preculture, followed by culturing at 37 °C with shaking (180 rpm) until an OD_{600} = 0.4 was reached. The cultures were cooled to 18 °C and protein expression was induced by addition of IPTG (400 mM in water, 1 mL L^{-1}). The expression cultures were shaken overnight at 18 °C and then centrifuged at 3.600 x g (4 °C). The supernatant was discarded and the cell pellet was resuspended in binding buffer (10 mL L^{-1} culture; 20 mM Na_2HPO_4, 500 mM NaCl, 20 mM imidazole, 1 mM $MgCl_2$, pH = 7.4, 4 °C). The resulting suspension was subjected to ultra-sonication (50 %, 5 x 1 min, on ice) for cell lysis. The cell debris was removed by centrifugation (14.610 x g, 2 x 7 min, 4 °C) and the supernatant was loaded onto a Ni^{2+}-NTA affinity chromatography column (Super Ni-NTA, Generon, Slough, UK). The column was washed with binding buffer (2 x 10mL L^{-1} culture), and the desired His-tagged protein was eluted using elution buffer (10 mL L^{-1} culture, 20 mM Na_2HPO_4, 500 mM NaCl, 500 mM imidazole, 1 mM $MgCl_2$, pH = 7.4, 4 °C). Fractions containing protein were analysed by SDS-PAGE (Figure S3) and used for incubation experiments. Protein concentrations were determined by Bradford assay calibrated to bovine serum albumin.[16]

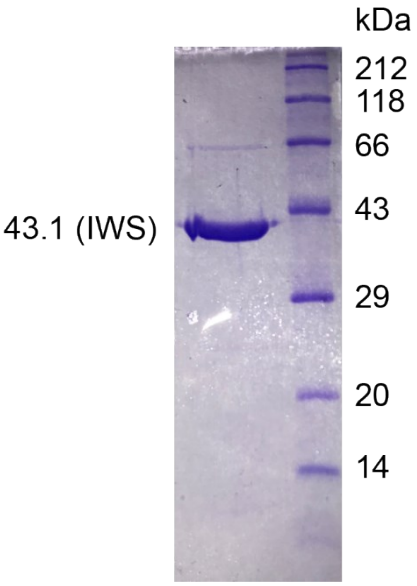

Figure S3. SDS-PAGE analysis of purified IWS (left lane). The right lane shows a mixture of protein standards of indicated sizes for comparison.

Incubation experiments

Test incubations were performed with GPP, FPP, GGPP and GFPP (0.2 mg each) dissolved in substrate buffer (100 µL; 25 mM NH_4HCO_3). After dilution with incubation buffer (0.4 mL; 50 mM Tris/HCl, 10 mM $MgCl_2$, 20% glycerol, pH = 8.2), IWS elution fraction (0.5 mL, ca. 0.5 mg mL^{-1}) was added. The reaction mixtures were incubated at 28 °C with shaking for 3 h, followed by extraction with hexane (150 µL). The organic layers were dried with $MgSO_4$ and analysed by GC/MS. Terpene production was only observed in the experiment with FPP (Figure 1 of main text).

For a preparative scale incubation, FPP (80 mg) was dissolved in substrate buffer (20 mL), followed by addition of incubation buffer (200 mL). The reaction was started by addition of IWS elution fraction (100 mL) and incubated at 28 °C for 3 h. The reaction mixture was extracted with Et_2O (3x 200 mL), the organic layers were dried with $MgSO_4$ and concentrated under reduced pressure. Column chromatography on silica gel with pentane yielded the sesquiterpene hydrocarbon **1** (1.0 mg) as a colourless oil.

GC/MS analyses

GC/MS analyses were carried out using a 7890B GC equipped with a HP5-MS fused silica capillary column (30 m, 0.25 mm i. d., 0.50 μm film) and connected to a 5977A mass detector (Agilent). GC parameters: 1) temperature program: 5 min at 50 °C increasing at 5 °C min^{-1} to 320 °C, 2) injection volume: 2 μL, 3) split ratio: 10:1, 60 s valve time, and 4) carrier gas: He at 1 mL min^{-1}. Retention indices (*I*) were determined from a homologous series of *n*-alkanes (C_7-C_{40}). MS parameters: 1) inlet pressure: 77.1 kPa, He at 23.3 mL min^{-1}, 2) transfer line: 250 °C, and 3) electron energy: 70 eV.

NMR spectroscopy

NMR spectra were recorded on a Bruker (Billerica, MA, USA) Avance III HD Cryo (700 MHz) NMR spectrometer. Spectra were measured in C_6D_6 and referenced against solvent signals (^{1}H-NMR, residual proton signal: δ = 7.16; ^{13}C-NMR: δ = 128.06).[17]

GC/MS-QTOF

GC/MS-QTOF analyses were recorded using a 7890B GC connected to a 7200 accurate-mass Q-TOF detector (Agilent). The GC was equipped with a HP5-MS fused silica capillary column (30 m, 0.25 mm i. d., 0.50 μm film). GC parameters: 1) temperature program: 5 min at 50 °C increasing at 5 °C min^{-1} to 320 °C, 2) injection volume: 1 μL, 3) split ratio: 50:1, 60 s valve time, and 4) carrier gas: He at 1 mL min^{-1}. MS parameters were 1) inlet pressure: 83.2 kPa, He at 24.6 mL min^{-1}, 2) transfer line: 250 °C, 3) electron energy 70 eV.

IR spectroscopy and optical rotations

IR spectra were recorded on an Alpha II FTIR spectrometer (Bruker Optics, MA, USA) with a scan range of 500 – 4000 cm^{-1}. Optical rotations were determined with a MCP 150 Modular Circular Polarimeter (Anton Paar GmbH, Graz, Austria).

(+)-Isoishwarane (**1**). TLC (pentane): R_f = 0.83. Optical rotation: $[\alpha]_D^{20}$ = +4.4 (*c* 0.52, benzene). HRMS (ToF): *m*/*z* = 204.1875 (calc. for $[C_{15}H_{24}]^{+\cdot}$ 204.1873). GC (HP-5MS): *I* = 1459. MS (EI, 70 eV): Figure 1 of main text. IR (diamond ATR): ν / cm^{-1} = 2955 (m), 2924 (s), 2855 (m), 1665 (w), 1462 (w), 1378 (w), 1261 (w), 1096 (w), 1018 (w), 799 (w) (Figure S11). NMR data are given in Table 1 of main text and Figures S4–S10.

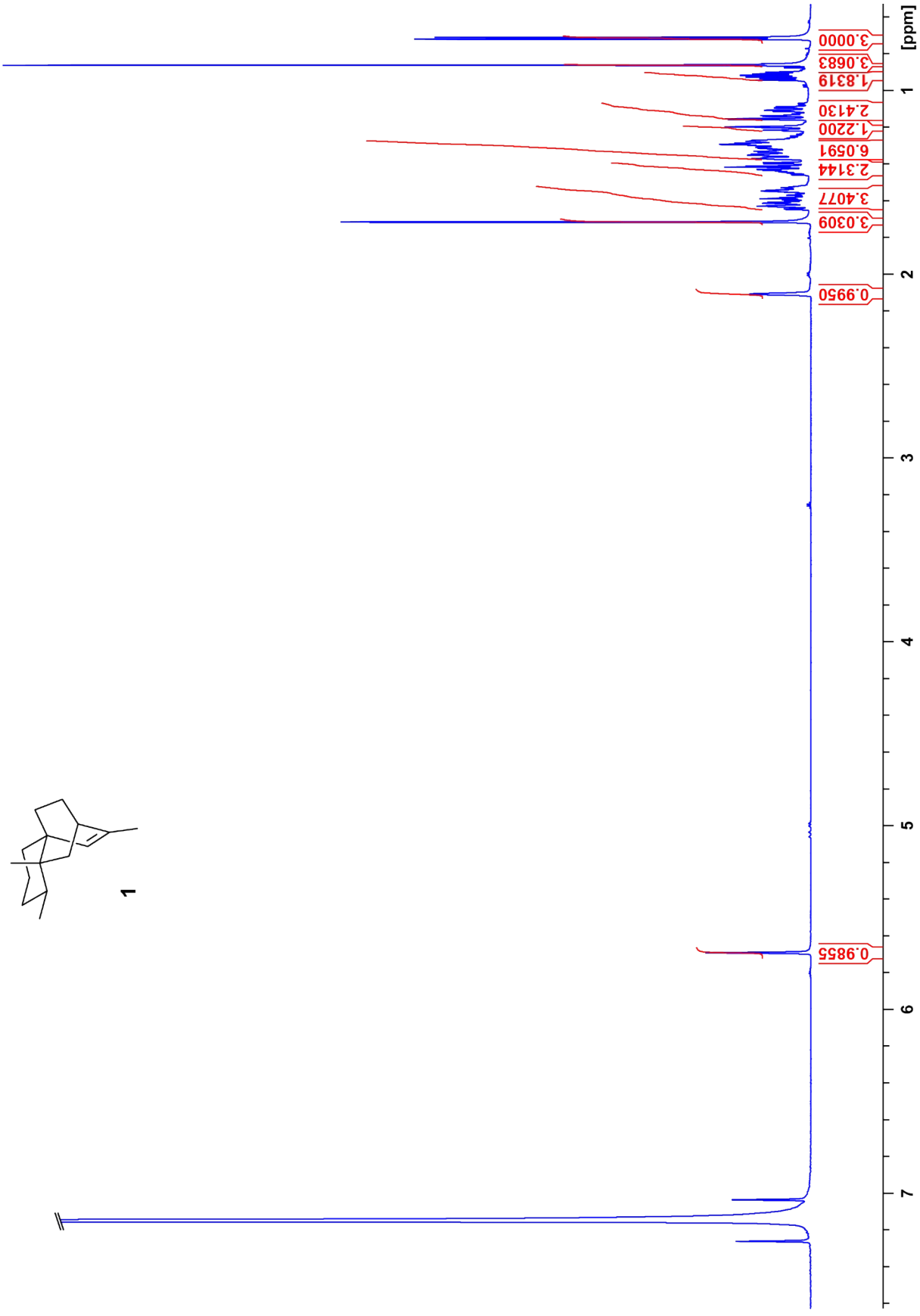

Figure S4. ^{1}H-NMR spectrum (700 MHz, C_6D_6) of **1**.

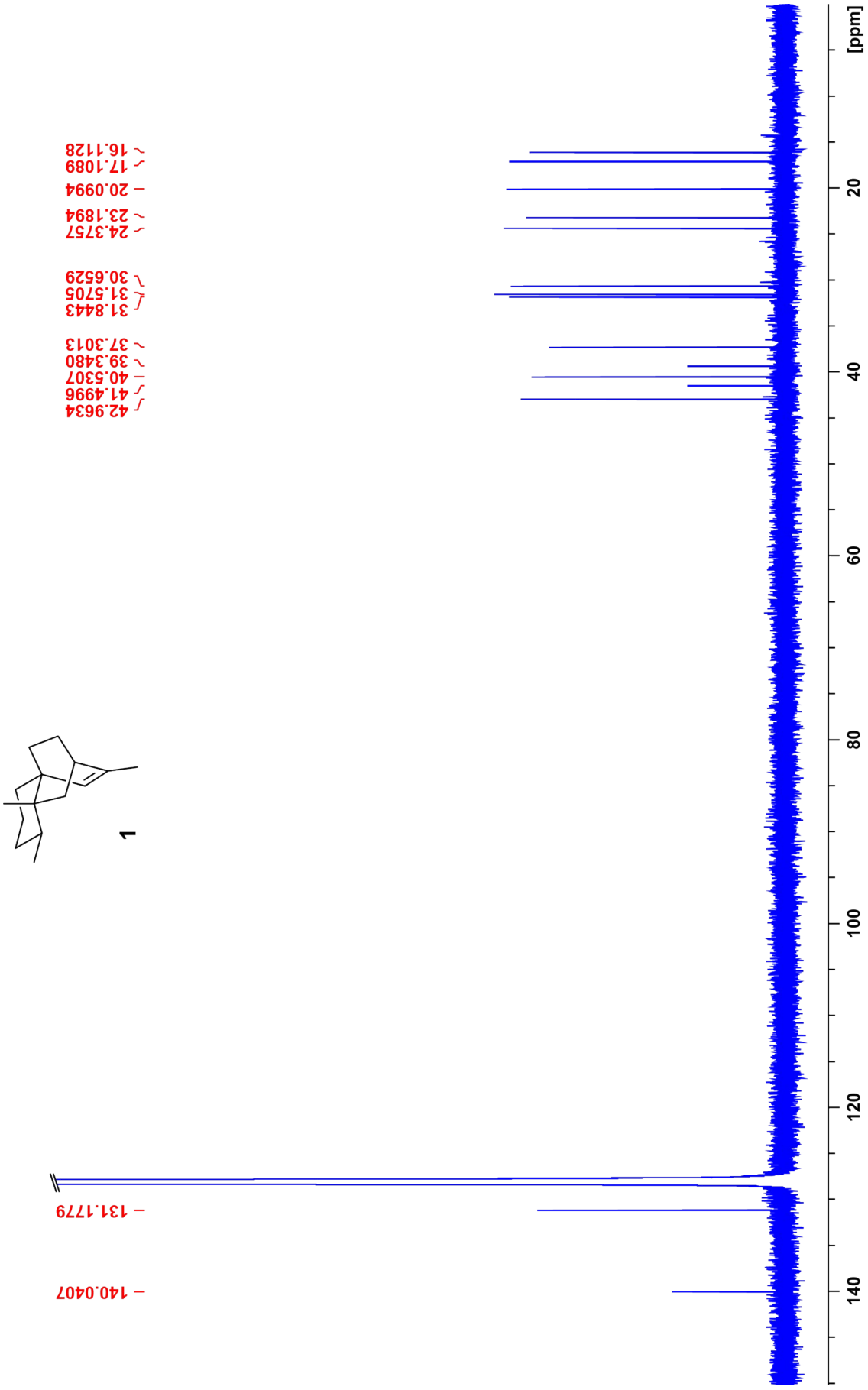

Figure S5. ^{13}C-NMR spectrum (176 MHz, C_6D_6) of **1**.

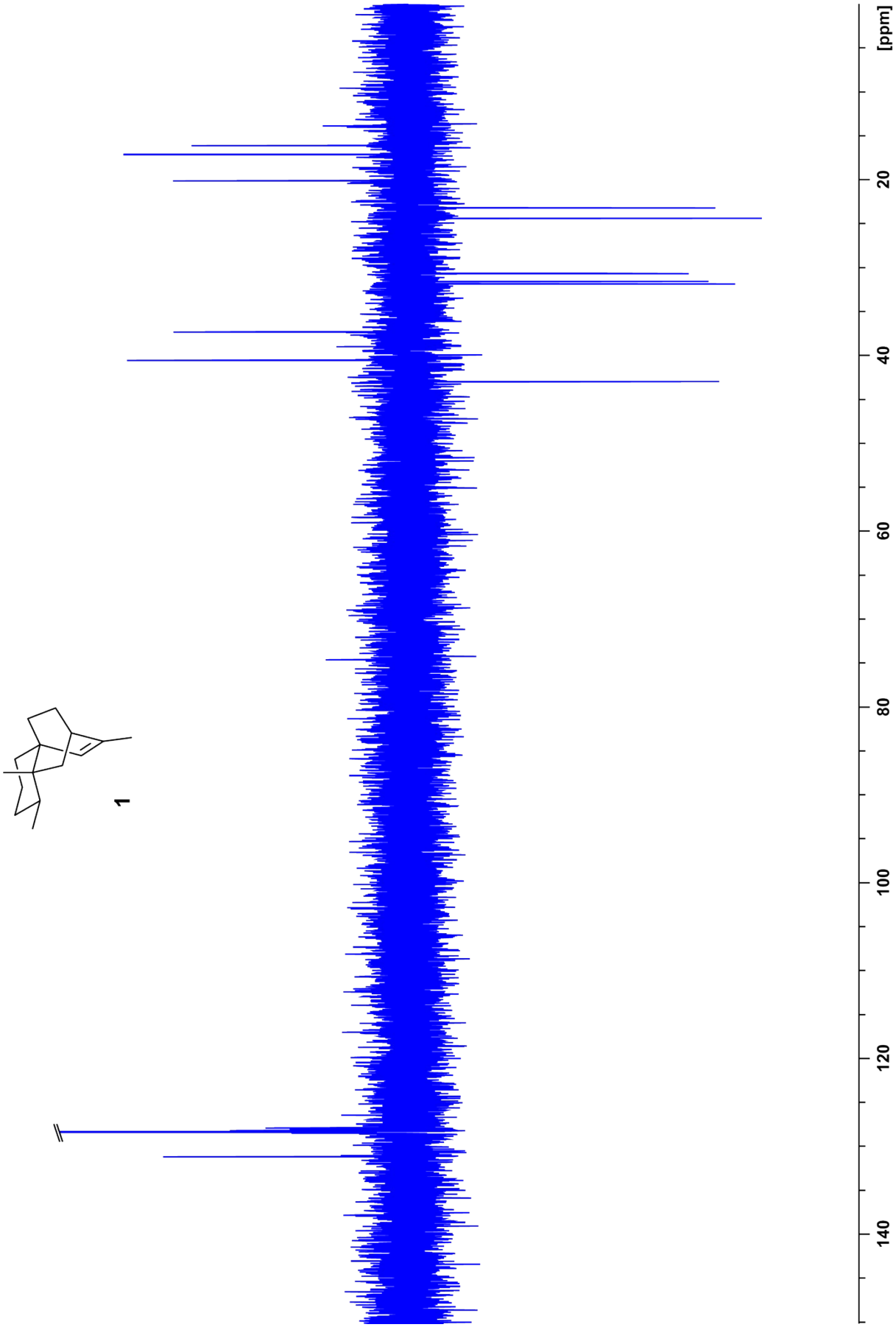

Figure S6. ^{13}C-DEPT135 spectrum (176 MHz, C_6D_6) of **1**.

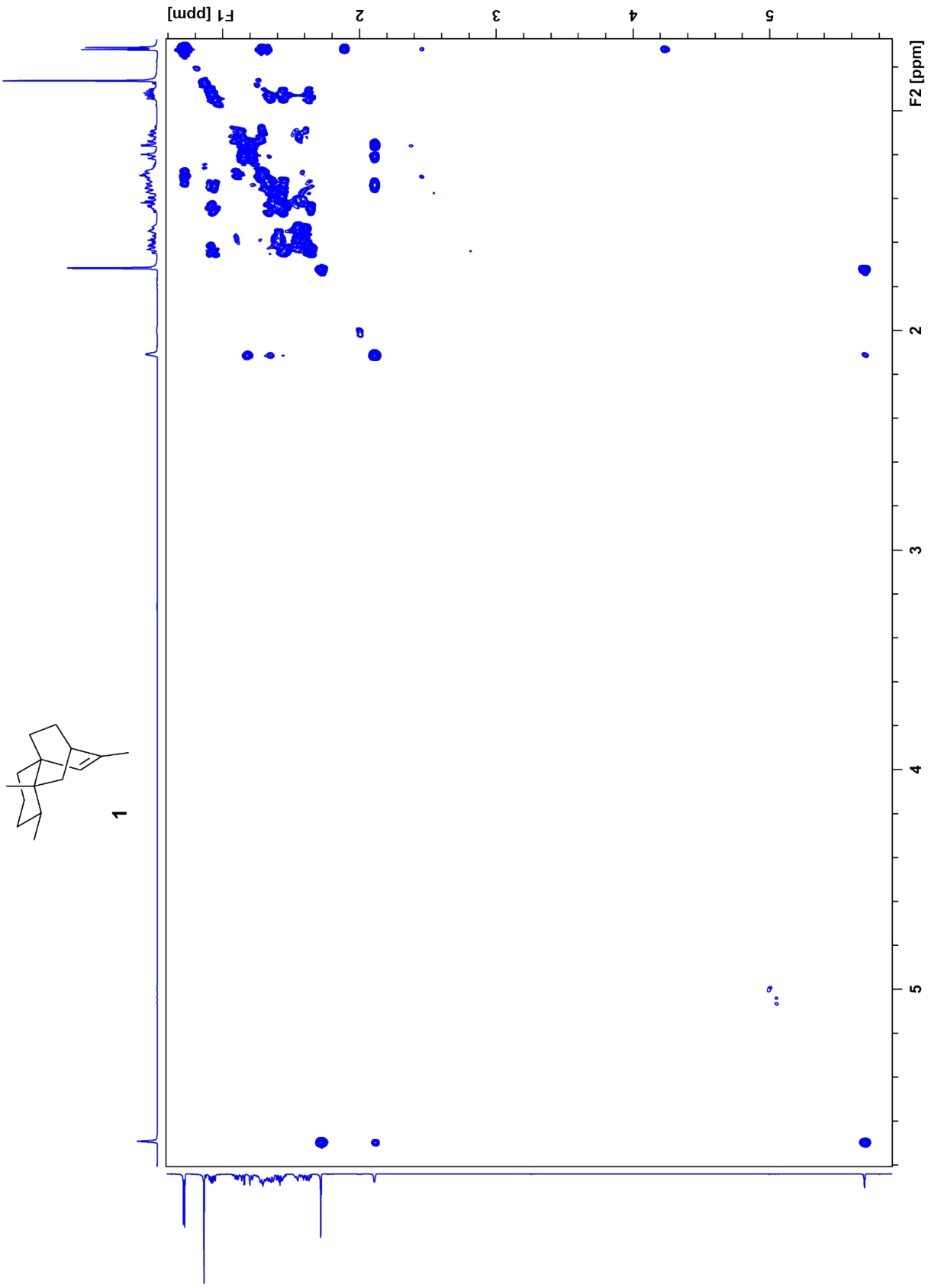

Figure S7. $^{1}H,^{1}H$-COSY spectrum (C_6D_6) of **1**.

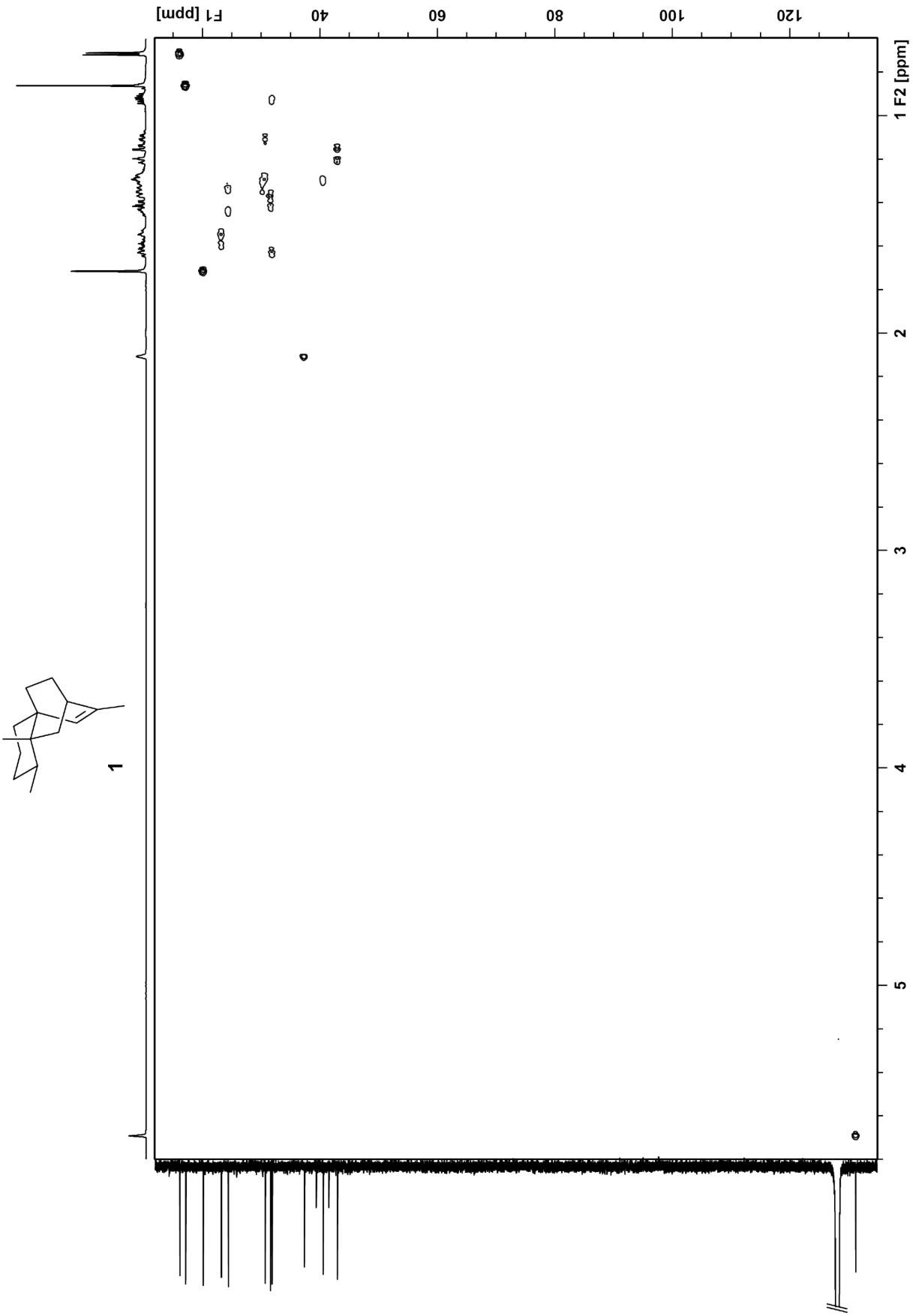

Figure S8. HSQC spectrum (C_6D_6) of **1**.

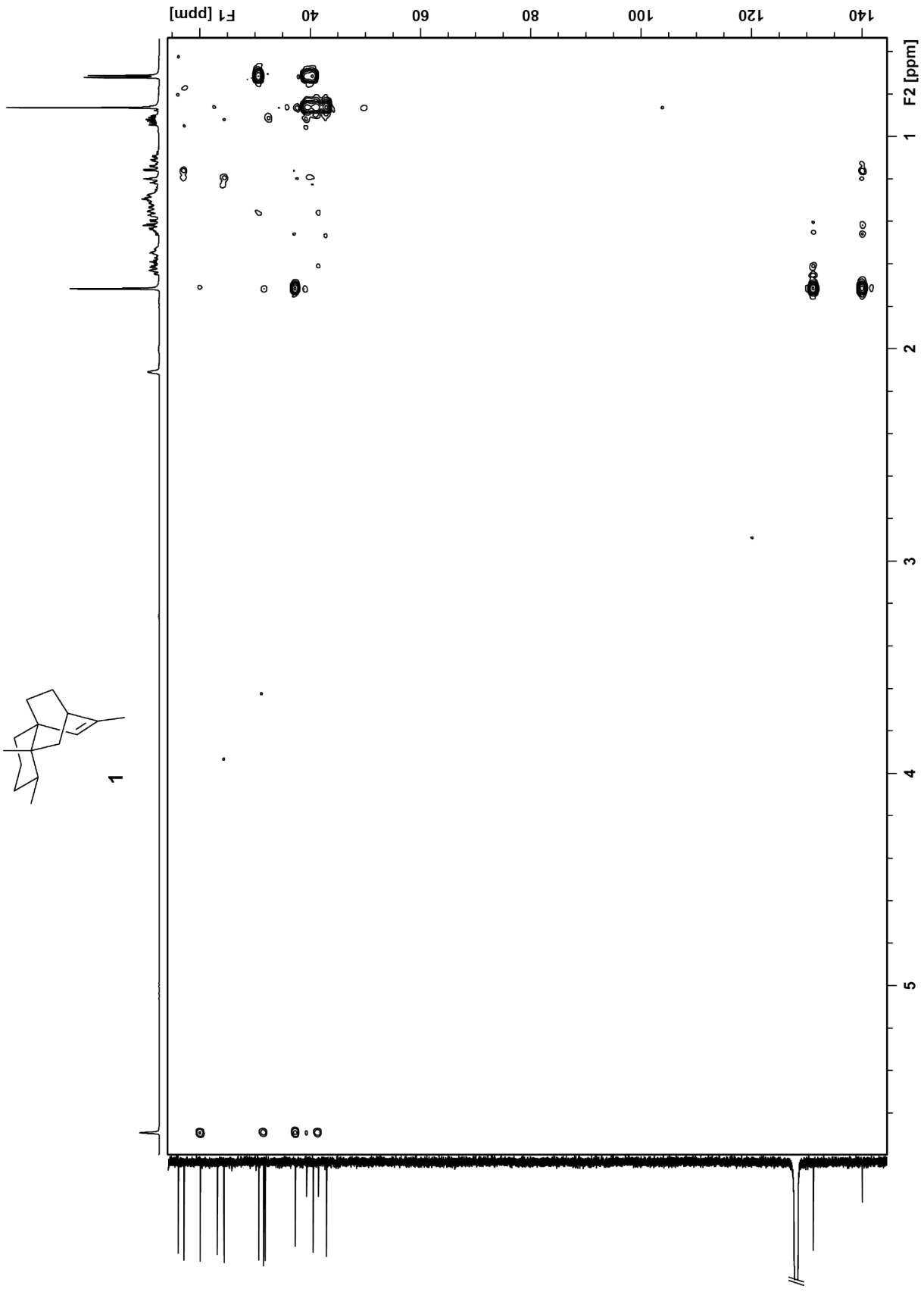

Figure S9. HMBC spectrum (C_6D_6) of **1**.

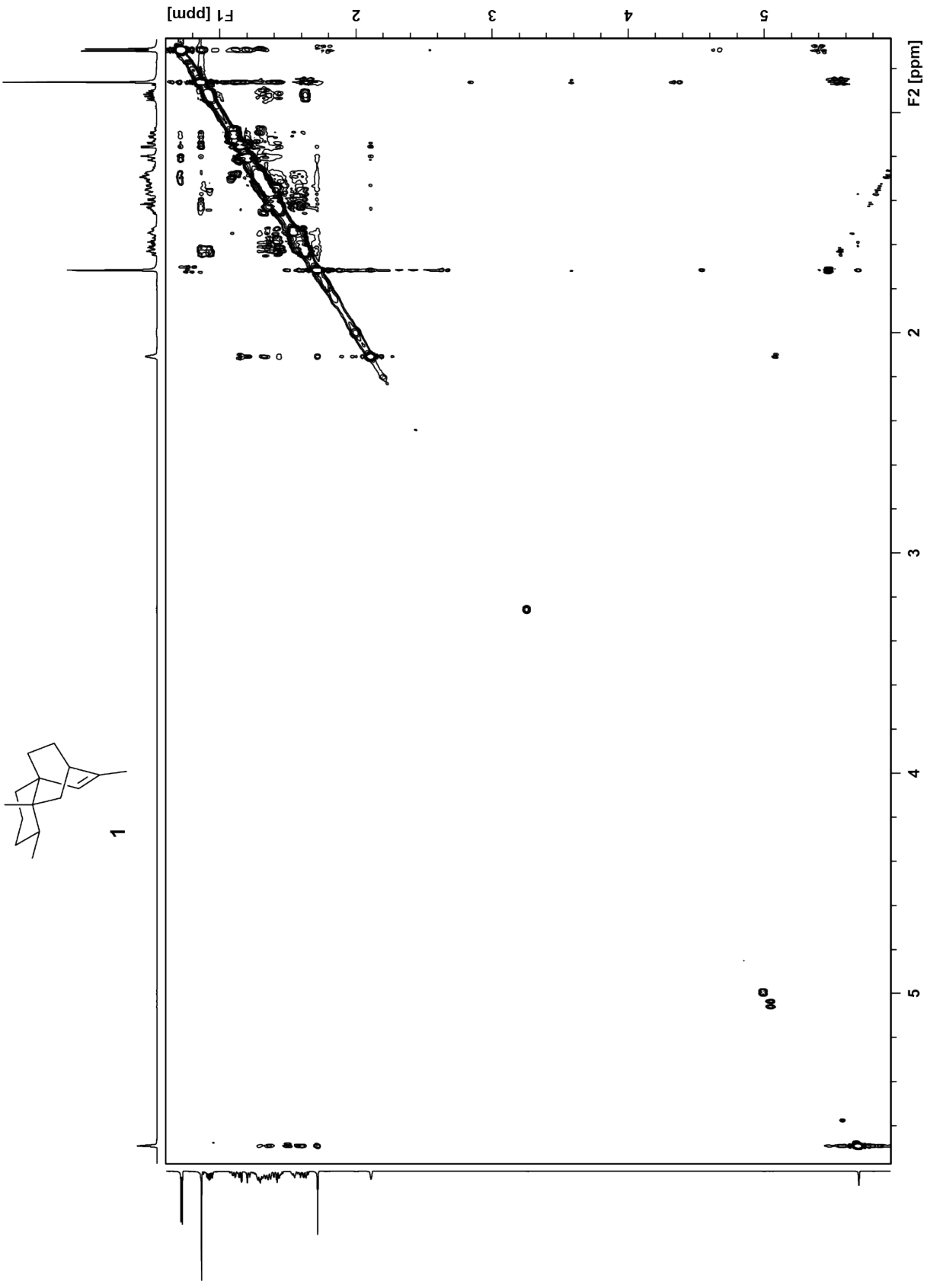

Figure S10. NOESY spectrum (C_6D_6) of **1**.

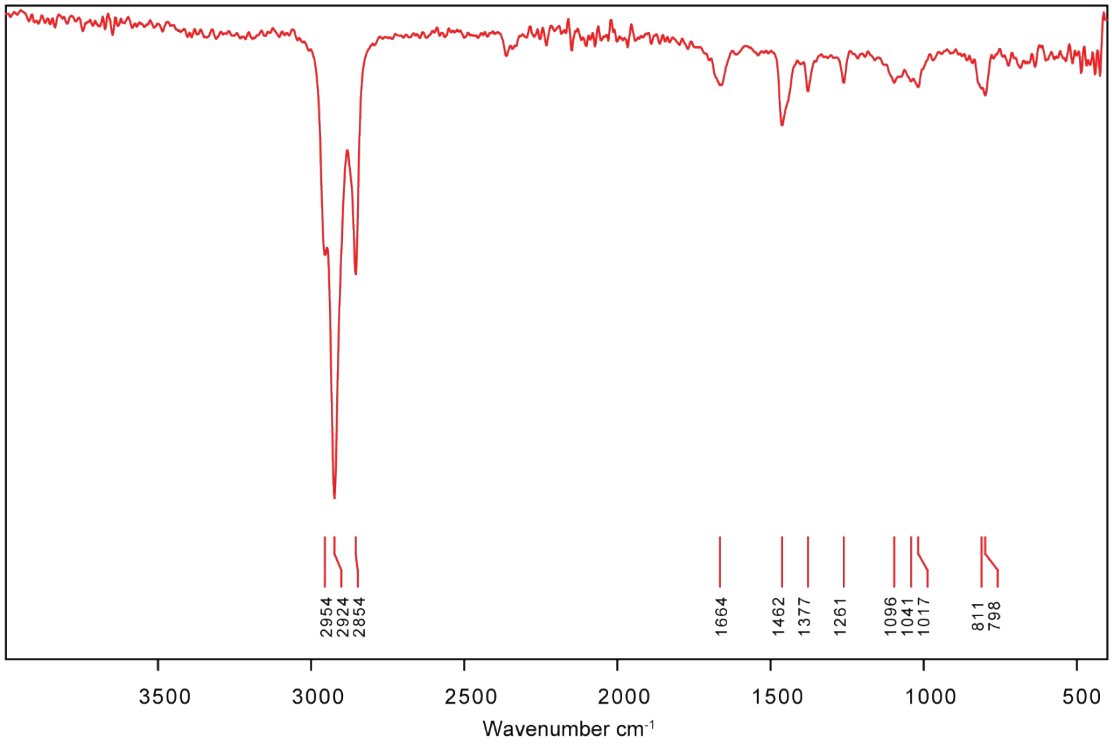

Figure S11. IR spectrum of **1**.

Incubation experiments with labelled substrates and substrate analogs

Isotopic labelling experiments and experiments with non-natural substrate analogs were performed with substrates (ca. 1 mg each) dissolved in substrate buffer (1 mL). Incubation buffer (5 mL) and enzyme elution fractions (2 mL for each enzyme) were added. For combinations of substrates and enzymes cf. Table S2. After incubation with shaking at 28 °C for 3 h the products were extracted with C_6D_6 twice (650 μL and 300 μL). The combined extracts were dried with $MgSO_4$ and analysed by NMR and/or GC/MS.

Table S2. Labelling experiments with IWS.

entry	substrate(s)	enzyme(s)	results shown in
1	(*R*)-(1-^{13}C,1-^{2}H)IPP[1]	IDI,[1] FPPS,[18] IWS	Figures 2, S12 and S13
2	(*S*)-(1-^{13}C,1-^{2}H)IPP[1]	IDI,[1] FPPS,[18] IWS	Figures 2, S12 and S13
3	DMAPP + (*E*)-(4-^{13}C,4-^{2}H)IPP[19]	FPPS,[18] IWS	Figure S14
4	DMAPP + (*Z*)-(4-^{13}C,4-^{2}H)IPP[19]	FPPS,[18] IWS	Figure S14
5	(1-^{13}C)FPP[20]	IWS	Figures 4 and S19
6	(2-^{13}C)FPP[20]	IWS	Figures 4 and S19
7	(3-^{13}C)FPP[20]	IWS	Figures 4 and S19
8	(4-^{13}C)FPP[20]	IWS	Figures 4 and S19
9	(5-^{13}C)FPP[20]	IWS	Figures 4 and S19
10	(6-^{13}C)FPP[20]	IWS	Figures 4 and S19
11	(7-^{13}C)FPP[20]	IWS	Figures 4 and S19
12	(8-^{13}C)FPP[20]	IWS	Figures 4 and S19
13	(9-^{13}C)FPP[20]	IWS	Figures 4 and S19
14	(2-^{13}C)DMAPP[21] + IPP	FPPS,[18] IWS	Figures 4 and S19
15	(11-^{13}C)FPP[20]	IWS	Figures 4 and S19
16	(12-^{13}C)FPP[20]	IWS	Figures 4 and S19
17	(9-^{13}C)GPP[22] + IPP	FPPS,[18] IWS	Figures 4 and S19
18	(10-^{13}C)GPP[23] + IPP	FPPS,[18] IWS	Figures 4 and S19
19	(15-^{13}C)FPP[20]	IWS	Figures 4 and S19
20	(6-^{13}C)FPP[20] in $^{2}H_2O$	IWS	Figure 5
21	(2-^{2}H)GPP[22] + IPP	FPPS,[18] IWS	Figure S17
22	(3-^{13}C,2-^{2}H)FPP[24]	IWS	Figure 5

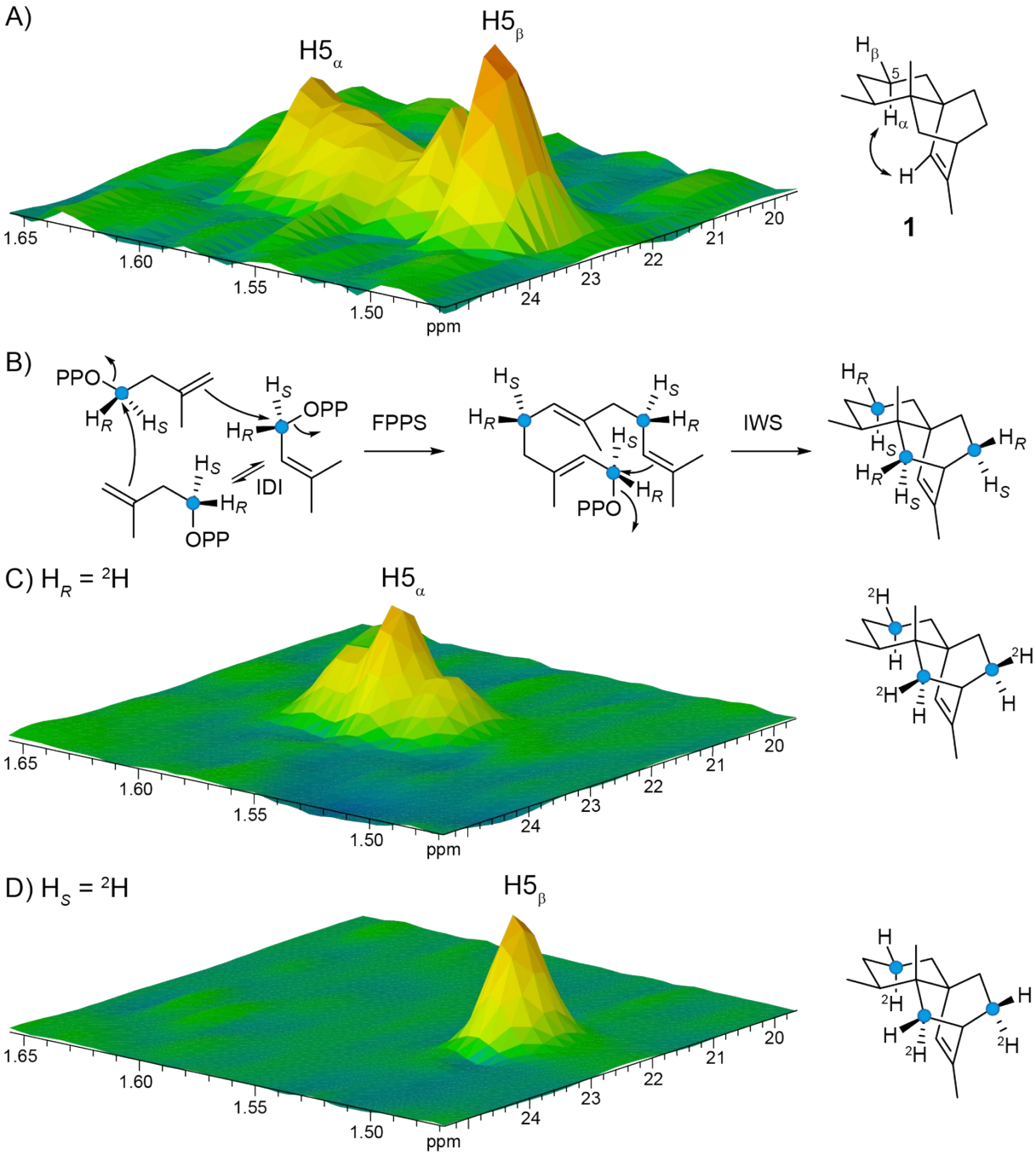

Figure S12. Absolute configuration of **1**. A) Partial HSQC of unlabelled **1** showing the signals for the diastereotopic hydrogens connected to C5. B) Formation of labelled **1** from (*R*)- and (*S*)-(1-^{13}C,1-^{2}H)IPP with IDI, FPPS and IWS (for brevity successive IPP additions to DMAPP are shown in one step without showing the intermediate GPP). HSQC spectra for C5 of labelled **1** obtained from C) (*R*)-(1-^{13}C,1-^{2}H)IPP and D) from (*S*)-(1-^{13}C,1-^{2}H)IPP. As a result of the enantioselective deuteration, in each labelling experiment one of the two crosspeaks is vanished, while the second crosspeak shows a slight upfield shift for both δ_H and δ_C. The known absolute configuration at C5 of the labelled compounds together with the NOESY based assignment of relative orientations of hydrogens, cf. double headed arrow in A), allows to conclude on the absolute configuration of **1** as shown.

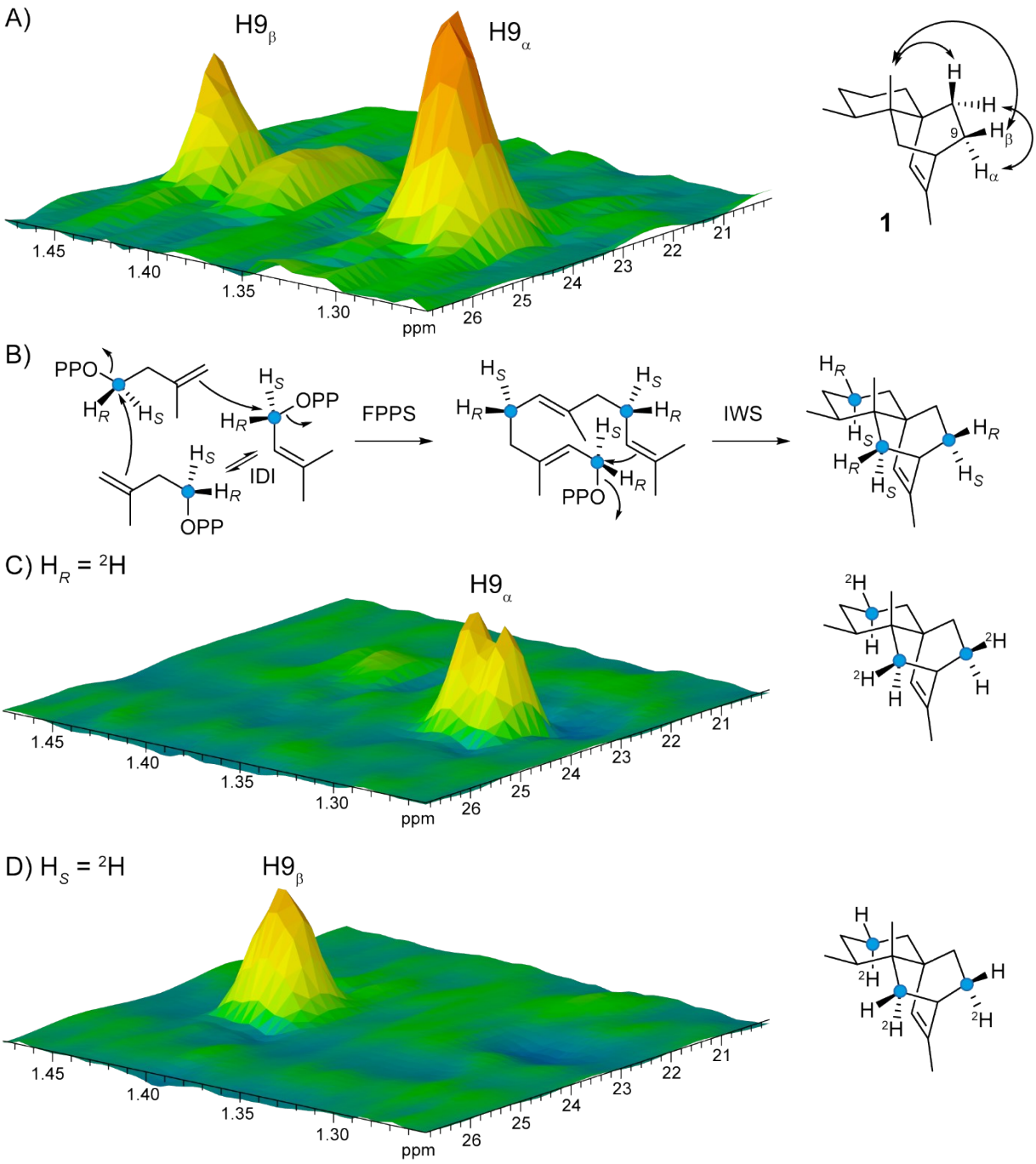

Figure S13. Absolute configuration of **1**. A) Partial HSQC of unlabelled **1** showing the signals for the diastereotopic hydrogens connected to C9. B) Formation of labelled **1** from (*R*)- and (*S*)-(1-^{13}C,1-^{2}H)IPP with IDI, FPPS and IWS (for brevity successive IPP additions to DMAPP are shown in one step without showing the intermediate GPP). HSQC spectra for C9 of labelled **1** obtained from C) (*R*)-(1-^{13}C,1-^{2}H)IPP and D) from (*S*)-(1-^{13}C,1-^{2}H)IPP. As a result of the enantioselective deuteration, in each labelling experiment one of the two crosspeaks is vanished, while the second crosspeak shows a slight upfield shift for both δ_H and δ_C. The known absolute configuration of the labelled compounds at C9 together with the NOESY based assignment of relative orientations of hydrogens, cf. double headed arrows in A), allows to conclude on the absolute configuration of **1** as shown.

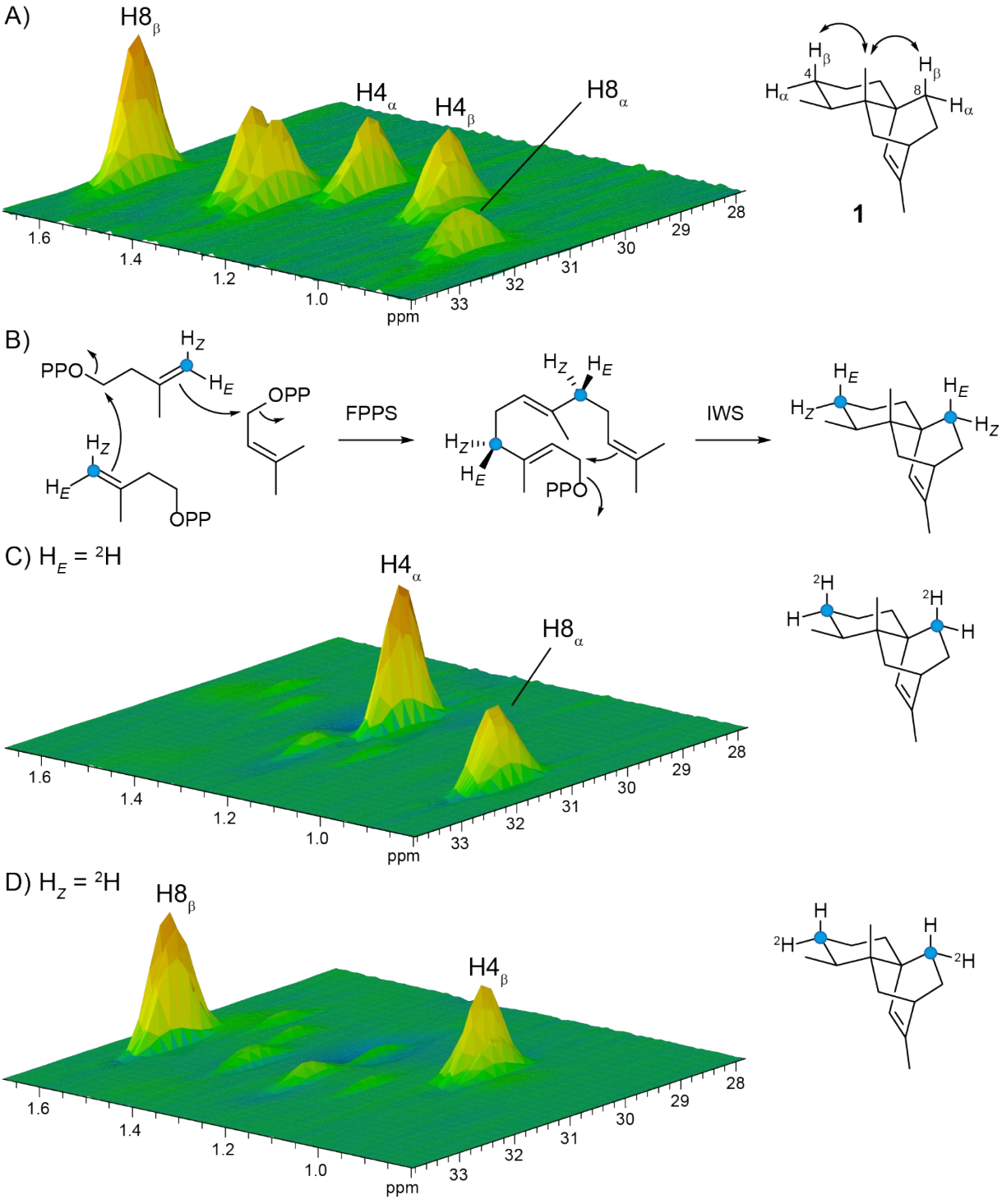

Figure S14. Absolute configuration of **1**. A) Partial HSQC of unlabelled **1** showing the signals for the diastereotopic hydrogens connected to C4 and C8. B) Formation of labelled **1** from (*E*)- and (*Z*)-(4-^{13}C,4-^{2}H)IPP and DMAPP with FPPS and IWS (for brevity successive IPP additions to DMAPP are shown in one step without showing the intermediate GPP). HSQC spectra for C4 and C8 of labelled **1** obtained from C) (*E*)-(4-^{13}C,4-^{2}H)IPP and D) from (*Z*)-(4-^{13}C,4-^{2}H)IPP. As a result of the enantioselective deuteration, in each labelling experiment one of the two crosspeaks for C4 and C8 is vanished, while the second crosspeak shows a slight upfield shift for both δ_H and δ_C. The known absolute configuration of the labelled compounds at C4 and C8 together with the NOESY based assignment of relative orientations of hydrogens, cf. double headed arrows in A), allows to conclude on the absolute configuration of **1** as shown.

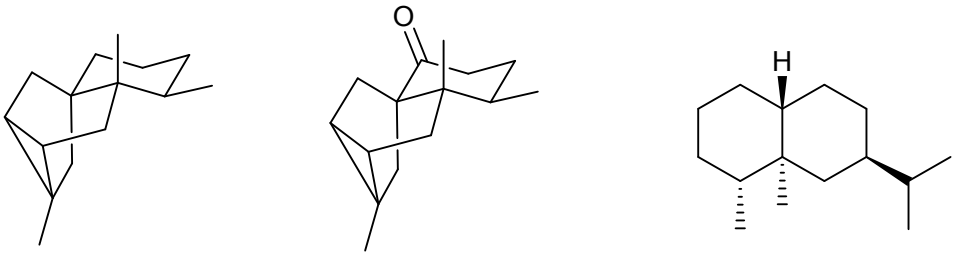

ishwarane ishwarone (+)-nootkatane

Figure S15. Structures of ishwarane, ishwarone and (+)-nootkatane.

GC analyses using a chiral stationary phase

Enantioselective GC analyses were performed with an Agilent 7820A GC system (Agilent, Santa Clara, CA, USA) equipped with a flame ionisation detector (FID) and an Agilent Cyclosil-B capillary column (30 m, 0.25 mm i. d., 0.25 μm film). The GC program was: starting from 80 °C, increasing with 2.5 °C/min to 220 °C, then hold for 5 min. Inlet temperature was 250 °C, inject volume was 1 μL, the split mode was splitless and the carrier gas was H_2 at a gas flow of 2.3 mL/min.

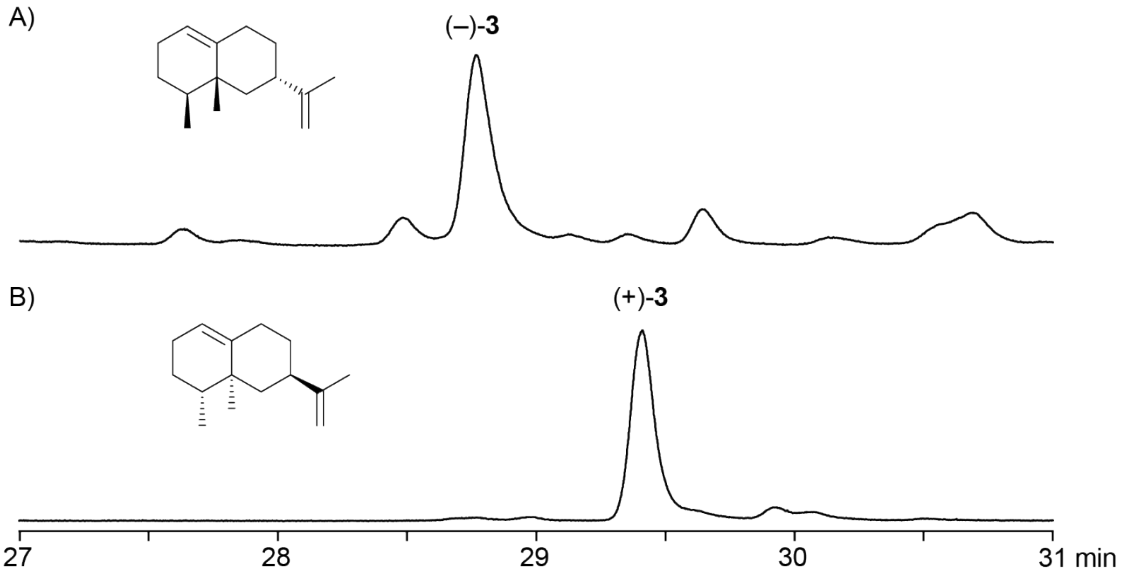

Figure S16. Determination of the absolute configuration of **3** by GC using a chiral stationary phase. A) GC analysis of a crude extract obtained by enzymatic conversion of FPP with IWS. The partial chromatogram shows the region for the elution of **3**. B) GC analysis of (+)-**3** from orange, showing a clearly different retention time to **3** from IWS. In conclusion, the enzyme product from IWS is identified as (–)-**3**.

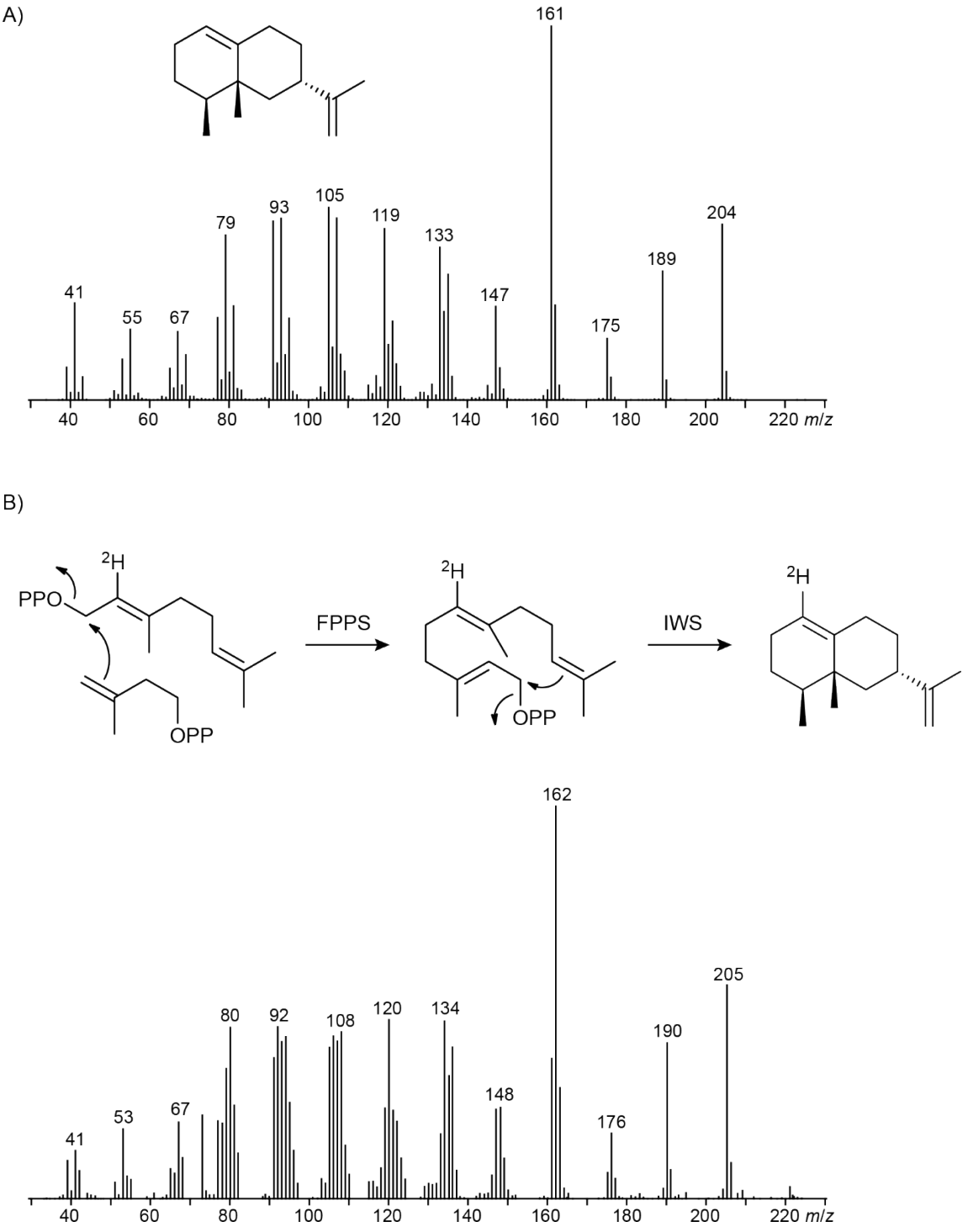

Figure S17. Deprotonation from C6 in the formation of **3**. A) EI mass spectrum of unlabelled **3**. B) Enzymatic conversion of (2-^{2}H)GPP and IPP with FPPS and IWS results in deuterated **3** as indicated by the obtained EI mass spectrum, confirming that the deprotonation from C6 proceeds with removal of the same proton as introduced in the protonation of **2** to **B** (Scheme 1 of main text).

Table S3. Newly identified highly conserved amino acid residues in bacterial type I terpene synthases.

Terpene synthase	No.[a]	Ref.	MTS[b]	STS	DTS	StTS	77[c]	%[d]	84[c]	%[d]	126[c]	%[d]	229[c]	%[d]
Isoishwarane	6	this work		x			F	100	T	100	N D	17 83	L	100
Linalool	15	[25]	x				A	100	D	100	L	100	K	100
(*R*)-Linalool/Nerolidol	2	[26]	x				F	100	D	100	D	100	K	100
1,8-Cineol	1	[27]	x				F	100	D	100	D	100	K	100
(+)-*epi*-Cubenol	148	[3]		x			F	100	D	100	D	99	K	100
(+)-T-Muurolol (II)	3	[4]		x			F	100	D	100	D	100	K	100
7-*epi*-α-Eudesmol	100	[4]		x			F	100	D	100	W	100	R	100
(–)-α-Amorphene	70	[4]		x			F	100	E	100	D	100	K	100
γ-Cadinene	15	[4]		x			F	100	D	100	D	87	K	100
Selina-4(15),7(11)-diene	82	[4]		x			F	100	C	100	D	100	KR	99
Avermitilol	35	[5]		x			F	100	D	100	D	100	K	100
Pentalenene	30	[6]		x			F	100	D	100	D	100	K	100
(+)-Isoafricanol	26	[7]		x			F	100	D	100	D	100	K	100
(+)-Dauc-8-en-11-ol	44	[8]		x			L	100	A	100	D	83	R	100
(–)-Neomeranol B	13	[8]		x			W	100	L	100	D	100	K	100
(+)-Intermedeol	7	[8]		x			W	100	L	100	DE	86	R	100
(+)-Caryolan-1-ol	125	[11]		x			F	98	D	100	G	87	K	100
(*E*)-β-Caryophyllene	1	[15]		x			F	100	D	100	D	100	K	100
(+)-4-*epi*-Cubebol	20	[15]		x			F	100	C	100	DE	90	K	100
(+)-Germacradien-6-ol	14	[20]		x			F	100	D	100	E	100	K	100
(+)-Pristinol	6	[24]		x			F	100	D	100	D	100	K	100
(–)-*epi*-α-Bisabolol	1	[28]		x			T	100	D	100	D	100	R	100
(–)-Germacradien-4-ol (I)	24	[28]		x			F	100	D	100	D	100	L	79
(–)-Germacradien-4-ol (II)	2	[29]		x			F	100	D	100	A	100	K	100
(+)-*epi*-Isozizaene	342	[30]		x			F	100	D	99	D	90	K	100

Terpene synthase	No.[a]	Ref.	MTS[b]	STS	DTS	StTS	77[c]	%[d]	84[c]	%[d]	126[c]	%[d]	229[c]	%[d]
epi-Zizaene	10	[31]		x			F	100	D	100	D	100	K	100
(2*Z*,6*E*)-Hedycaryol	1	[32]		x			F	100	D	100	A	100	R	100
(–)-δ-Cadinene	1	[33]		x			F	100	D	100	E	100	K	100
(+)-T-Muurolol (I)	1	[33]		x			F	100	C	100	D	100	K	100
(+)-Eremophilene	8	[34]		x			F	100	D	100	D	100	K	100
8-*epi*-α-Selinene	32	[35]		x			F	100	D	100	D	75	RK	100
10-*epi*-Cubebol	1	[36]		x			F	100	E	100	D	100	K	100
α-Selinene	1	[37]		x			F	100	D	100	D	100	K	100
Corvol ether	48	[38]		x			F	100	V	98	D	100	V	100
Germacrene A (I)	58	[1]		x			F	100	D	100	D	100	K	100
Germacrene A (II)	4	[35]		x			F	100	D	100	D	75	R	100
(+)-Allohedycaryol	7	[37]		x			F	100	D	100	D	100	K	100
Selina-3,7(11)-diene	10	[37]		x			F	100	C	100	D	100	K	100
(–)-Isohirsut-1-ene	1	[37]		x			F	100	D	100	D	100	K	100
(–)-Isohirsut-4-ene	18	[37]		x			F	100	D	100	D	100	K	100
African-2-ene	2	[37]		x			W	100	D	100	D	100	K	100
(*Z*)-γ-Bisabolene	1	[39]		x			F	100	D	100	D	100	R	100
β-Himachalene	1	[40]		x			F	100	D	100	N	100	K	100
Bungoene	9	[41]		x			F	100	D	100	D	100	K	100
Trichoacorenol	1	[42]		x			S	100	D	100	D	100	K	100
Cyclooctat-9-en-7-ol	21	[2]			x		F	100	D	100	D	100	R	100
Spiroviolene	30	[9]			x		F	100	D	100	DE	93	K	97
Micromonocyclol	116	[12]			x		F	100	DE	100	V	91	RK	93
Bonnadiene	1	[19]			x		T	100	D	100	D	100	K	100
Allokutznerene	3	[19]			x		F	100	D	100	D	100	K	100
Clavulatriene	1	[37]			x		F	100	E	100	D	100	K	100
Hydropyrene	1	[37]			x		Y	100	D	100	D	100	R	100
Obscuronatin	3	[37]			x		F	100	D	100	D	100	K	100

Terpene synthase	No.[a]	Ref.	MTS[b]	STS	DTS	StTS	77[c]	%[d]	84[c]	%[d]	126[c]	%[d]	229[c]	%[d]
Odyverdiene	1	[37]			x		F	100	C	100	D	100	R	100
Cyclooctat-7(8),10(14)-diene	1	[37]			x		G	100	D	100	D	100	R	100
Tsukubadiene	1	[37]			x		F	100	D	100	A	100	L	100
Cembrene C	4	[37]			x		F	100	D	100	D	100	K	100
18-Hydroxydolabella-3,7-diene	2	[43]			x		F	100	D	100	D	100	K	100
Catenul-14-en-6-ol	5	[44]			x		F	100	E	100	E	60	A	80
Cattleyene	4	[45]			x		F	100	D	100	D	100	K	100
Phomopsene (I)	5	[45]			x		F	100	D	100	D	100	K	100
Cembrene A	1	[46]			x		F	100	D	100	D	100	K	100
Spiroalbatene	2	[46]			x		S	100	D	100	E	100	K	100
Chryseodiene	4	[47]			x		M	100	E	100	A	100	K	100
Wanjudiene	19	[47]			x		A	100	D	100	L	100	K	100
Spata-13,17-diene	6	[48]			x		F	100	D	100	D	100	K	100
Spinodiene	1	[49]			x		W	100	D	100	T	100	N	100
Venezuelaene A	6	[50]			x		T	100	D	100	D	100	K	100
(*R*)-Nephthenol	1	[51]			x		F	100	E	100	D	100	K	100
Sestermobaraene	2	[52]				x	F	100	V	100	D	100	K	100

[a] Number of included sequences with high sequence homology, forming a monophyletic clade in a phylogenetic tree analysis, and thus presumably the same function as the characterised enzyme. [b] MTS: monoterpene synthase, STS: sesquiterpene synthase, DTS: diterpene synthase, and StTC: sesterterpene synthase. [c] Amino acid residues found in the indicated positions using IWS numbering. Amino acid residues deviating from the normal case are highlighted in red. [d] Percentage of cases in which the indicated amino acid is found for each group of homologous enzymes.

Site-directed mutagenesis

Single mutants were generated by three polymerase chain reaction (PCR) using pYE-IWS as a template and pairs of reverse complementary mutagenic primers (Table S1). For PCRs of mutant IWS_N126D, the first gene fragment was obtained using P1_fwd and N126D_rev as primers and the second gene fragment was obtained using P1_rev and N126D_fwd as primers. These two PCRs produced overlapping DNA fragments with the required mutation, which were used in the third PCR for elongation to a gene with full length. The homology arms were introduced by another PCR using the product of the third PCR as a template, and P2_fwd and P2_rev as primers. For the other single mutants, IWS_F77I, IWS_T84D and IWS_L229R, the required genes were generated using the same PCR method with corresponding primers. These PCR products were used for homologous recombination with linearised pYE-Express in yeast as described above. Plasmids were isolated and shuttled into E. coli BL21(DE3) by electroporation as described before. Then the single mutant plasmids were used as PCR templates for the production of double mutants. All variants were fully sequenced to verify the target mutation(s).

Expression and purification of enzyme variants

The expression and purification of each enzyme variant were conducted as described above. The protein concentrations were measured by Bradford assay. The enzyme concentrations (Table S4) and SDS-PAGE (Figure S18) are shown below.

Table S4. Enzyme yields of IWS and its mutants.

Wildtype	T84D	L229R	T84D L229R	N126D	F77I	F77I N126D	T84D N126D	N126D L229R
4.5 mg/mL	2.7 mg/mL	4.2 mg/mL	4.7 mg/mL	3.2 mg/mL	2.6 mg/mL	3.1 mg/mL	3.1 mg/mL	2.9 mg/mL

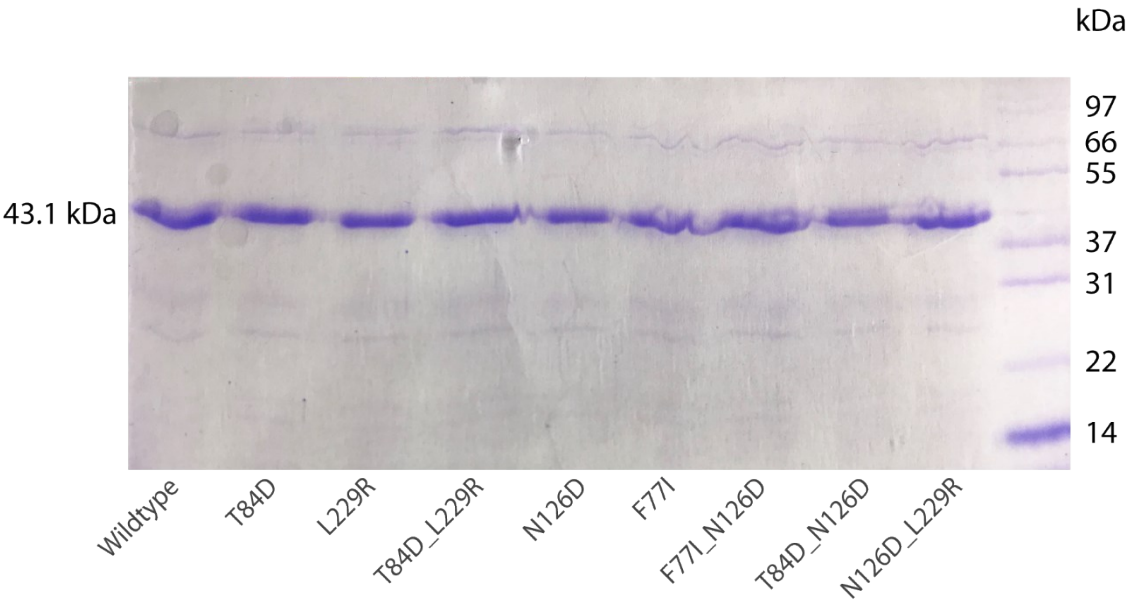

Figure S18. SDS-PAGE analyses of purified enzymes. The right line shows a mixture of protein standards of indicated sizes for comparison.

Activity tests with enzyme variants

All the enzymatic conversions of FPP were performed in a total volume of 1 mL, containing 0.5 mg FPP dissolved in 0.1 mL aqueous NH_4HCO_3 solution (25 mM), enzyme elution fraction in elution buffer (0.3 mL, enzyme concentrations adjusted to 2.6 mg/mL), binding buffer (0.1 mL) and incubation buffer (0.5 mL). After incubation with shaking at 28 °C overnight, the reaction mixtures were extracted with hexane (0.15 mL). The extracts were dried with $MgSO_4$ and analysed by GC/MS. Each enzymatic experiment was conducted in triplicates. The enzyme activity was assessed by peak integration of the product **1** and **2**.

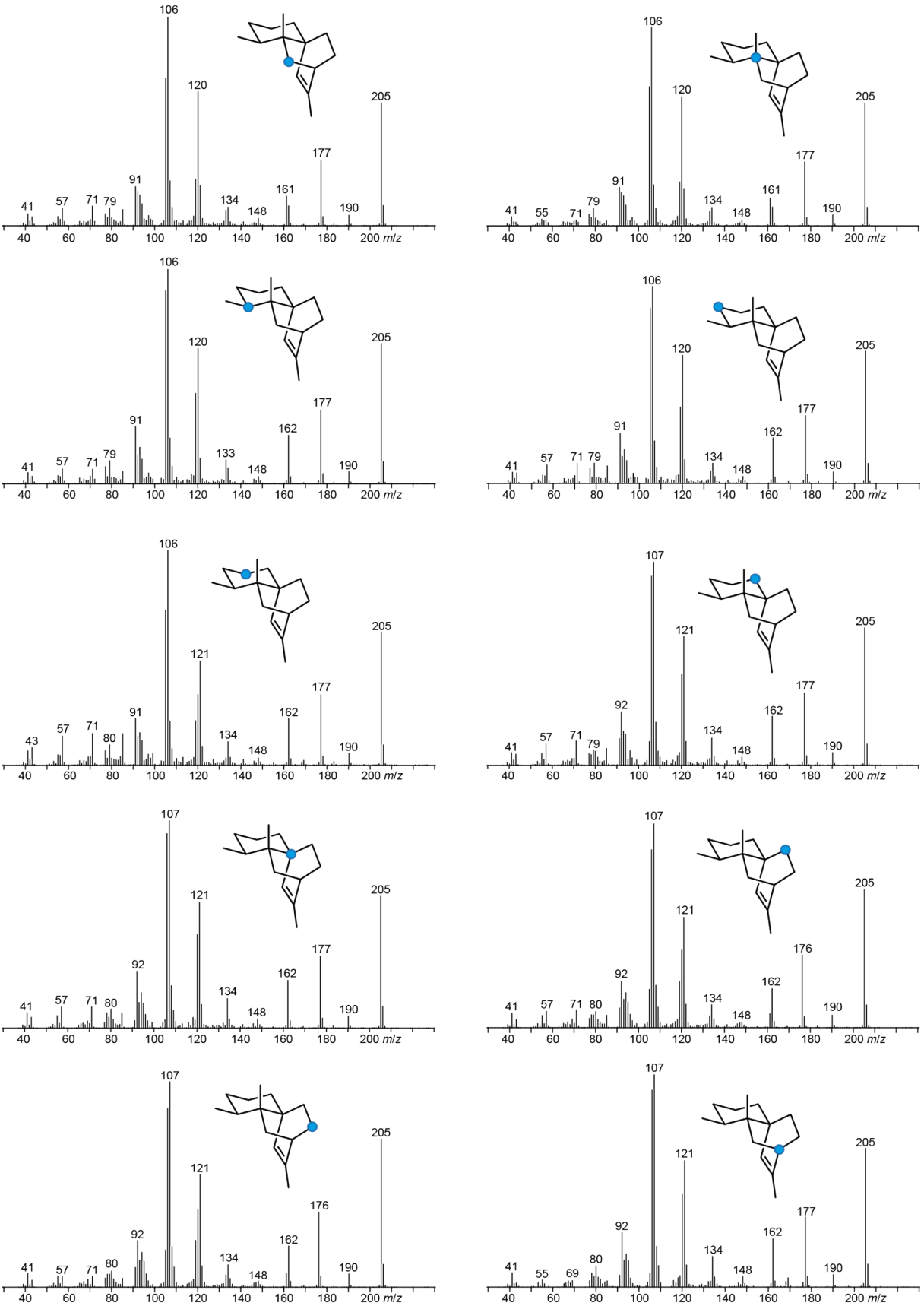

Figure S19. EI mass spectra of all 15 isotopomers of (^{13}C)-**1** obtained by enzymatic conversion of the corresponding 15 isotopomers of (^{13}C)FPP. Blue dots indicate ^{13}C-labelled carbons.

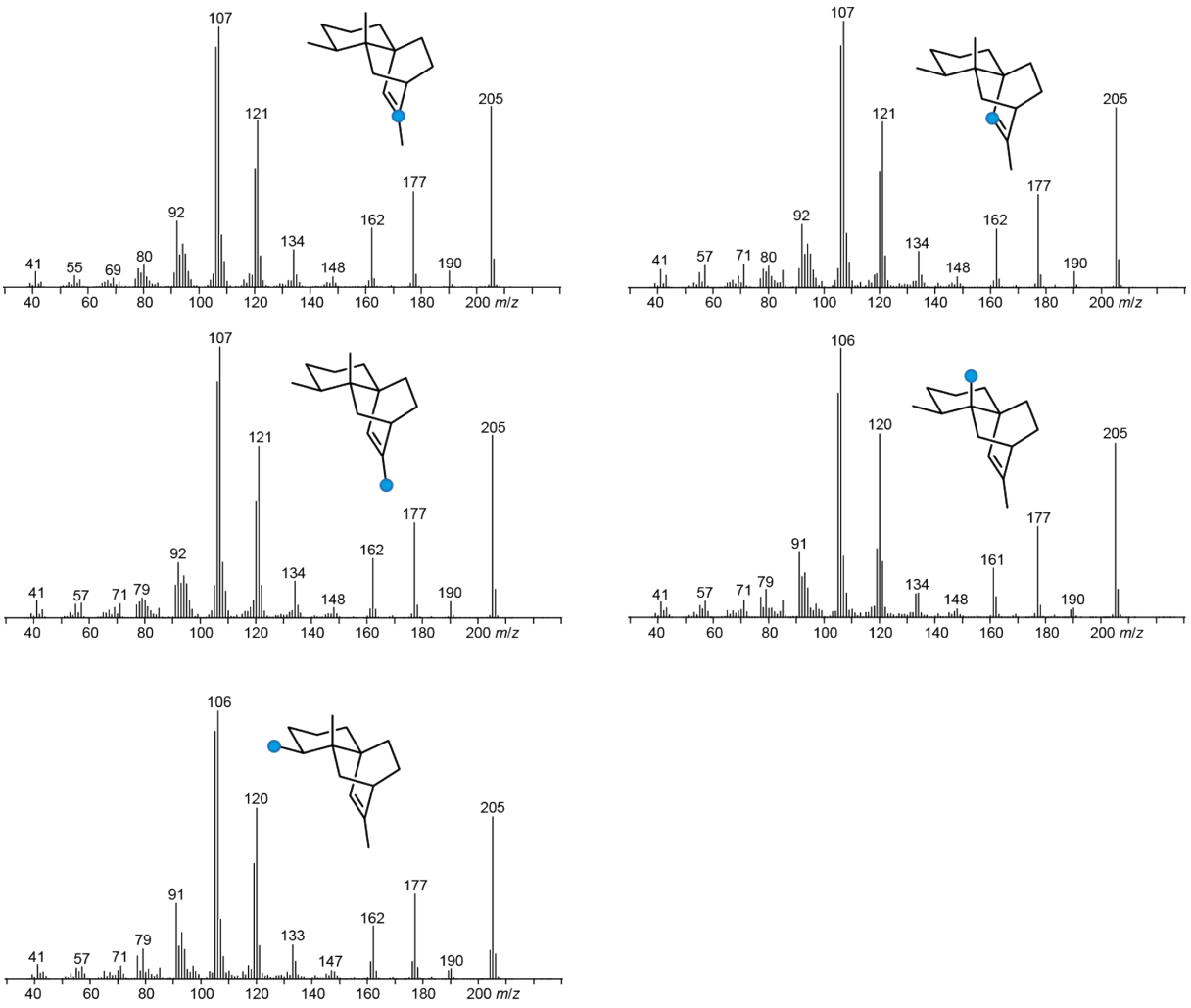

Figure S19. EI mass spectra of all 15 isotopomers of (^{13}C)-**1** obtained by enzymatic conversion of the corresponding 15 isotopomers of (^{13}C)FPP. Blue dots indicate ^{13}C-labelled carbons.

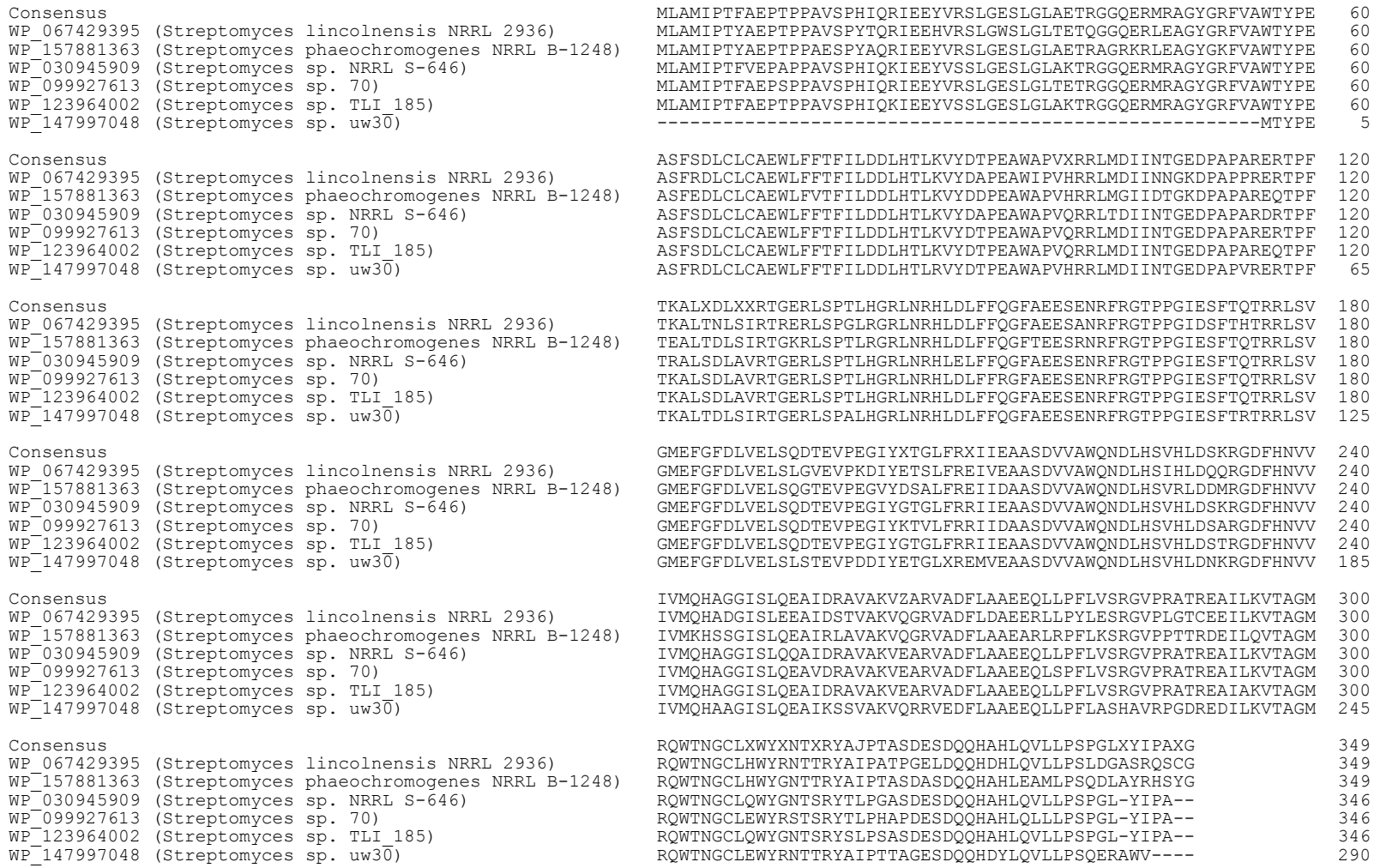

Figure S20. Alignment of IWS and five closely related homologs. Highly conserved motifs (from N- to C-terminus: Asp-rich motif, pyrophosphate sensor R, NSE triad, RY pair) are marked in yellow, residues mutated in the IWS from *S. lincolnensis* are marked in green.

References

[1] J. Rinkel and J. S. Dickschat, *Org. Lett.*, 2019, **21**, 2426.
[2] S.-Y. Kim, P. Zhao, M. Igarashi, R. Sawa, T. Tomita, M. Nishiyama and T. Kuzuyama, *Chem. Biol.*, 2009, **16**, 736.
[3] C. Nakano, T. Tezuka, S. Horinouchi and Y. Ohnishi, *J. Antibiot.*, 2012, **65**, 551.
[4] P. Rabe and J. S. Dickschat, *Angew. Chem. Int. Ed.*, 2013, **52**, 1810.
[5] W. K. W. Chou, I. Fanizza, T. Uchiyama, M. Komatsu, H. Ikeda and D. E. Cane, *J. Am. Chem. Soc.*, 2010, **132**, 8850.
[6] D. E. Cane, J. K. Sohng, C. R. Lamberson, S. M. Rudnicki, Z. Wu, M. D. Lloyd, J. S. Oliver and B. R. Hubbard, *Biochemistry*, 1994, **33**, 5846.
[7] P. Rabe, M. Samborskyy, P. F. Leadlay and J. S. Dickschat, *Org. Biomol. Chem.*, 2017, **15**, 2353.
[8] P. Rabe, J. Rinkel, T. A. Klapschinski, L. Barra and J. S. Dickschat, *Org. Biomol. Chem.*, 2016, **14**, 158.
[9] P. Rabe, J. Rinkel, E. Dolja, T. Schmitz, B. Nubbemeyer, T. H. Luu and J. S. Dickschat, *Angew. Chem. Int. Ed.*, 2017, **56**, 2776.
[10] P. Baer, P. Rabe, K. Fischer, C. A. Citron, T. A. Klapschinski, M. Groll and J. S. Dickschat, *Angew. Chem. Int. Ed.*, 2014, **53**, 7652.
[11] C. Nakano, S. Horinouchi and Y. Ohnishi, *J. Biol. Chem.*, 2011, **286**, 27980.
[12] J. Rinkel and J. S. Dickschat, *Org. Lett.*, 2019, **21**, 9442.
[13] X. Lin, R. Hopson and D. E. Cane, *J. Am. Chem. Soc.*, 2006, **128**, 6022.
[14] R. D. Giets and R. H. Schiestl, *Nat. Protoc.*, 2007, **2**, 31.
[15] J. S. Dickschat, K. A. K. Pahirulzaman, P. Rabe and T. A. Klapschinski, *ChemBioChem*, 2014, **15**, 810.
[16] M. M. Bradford, *Anal. Biochem.*, 1976, **72**, 248.
[17] G. R. Fulmer, A. J. M. Miller, N. H. Sherden, H. E. Gottlieb, A. Nudelman, B. M. Stoltz, J. E. Bercaw and K. I. Goldberg, *Organometallics*, 2010, **29**, 2176.
[18] P. Rabe, J. Rinkel, B. Nubbemeyer, T. G. Köllner, F. Chen and J. S. Dickschat, *Angew. Chem. Int. Ed.*, 2016, **55**, 15420.
[19] L. Lauterbach, J. Rinkel and J. S. Dickschat, *Angew. Chem. Int. Ed.*, 2018, **57**, 8280.
[20] P. Rabe, L. Barra, J. Rinkel, R. Riclea, C. A. Citron, T. A. Klapschinski, A. Janusko and J. S. Dickschat, *Angew. Chem. Int. Ed.*, 2015, **54**, 13448.
[21] J. Rinkel and J. S. Dickschat, *Beilstein J. Org. Chem.*, 2019, **15**, 1008.
[22] G. Bian, J. Rinkel, Z. Wang, L. Lauterbach, A. Hou, Y. Yuan, Z. Deng, T. Liu and J. S. Dickschat, *Angew. Chem. Int. Ed.*, 2018, **57**, 15887.
[23] T. Mitsuhashi, J. Rinkel, M. Okada, I. Abe and J. S. Dickschat, *Chem. Eur. J.*, 2017, **23**, 10053.
[24] T. A. Klapschinski, P. Rabe and J. S. Dickschat, *Angew. Chem. Int. Ed.*, 2016, **55**, 10141.
[25] A. Hou, L. Lauterbach and J. S. Dickschat, *Chem. Eur. J.*, 2020, **26**, 2178.
[26] C. Nakano, H.-K. Kim and Y. Ohnishi, *ChemBioChem*, 2011, **12**, 2403.
[27] C. Nakano, H.-K. Kim and Y. Ohnishi, *ChemBioChem*, 2011, **12**, 1988.
[28] C. Nakano, F. Kudo, T. Eguchi and Y. Ohnishi, *ChemBioChem*, 2011, **12**, 2271.
[29] J. Rinkel, P. Rabe, P. Garbeva and J. S. Dickschat, *Angew. Chem. Int. Ed.*, 2016, **55**, 13593.
[30] X. Lin, R. Hopson and D. E. Cane, *J. Am. Chem. Soc.*, 2006, **128**, 6022.
[31] C. A. Citron, J. Gleitzmann, G. Laurenzano, R. Pukall and J. S. Dickschat, *ChemBioChem*, 2012, **13**, 202.
[32] P. Baer, P. Rabe, C. A. Citron, C. C. de Oliveira Mann, N. Kaufmann, M. Groll and J. S. Dickschat, *ChemBioChem*, 2014, **15**, 213.
[33] Y. Hu, W. K. W. Chou, R. Hopson and D. E. Cane, *Chem. Biol.*, 2011, **18**, 32.
[34] A. Schifrin, T. T. B. Ly, N. Günnewich, J. Zapp, V. Thiel, S. Schulz, F. Hannemann, Y. Khatri and R. Bernhardt, *ChemBioChem*, 2015, **16**, 337.
[35] S. A. Agger, F. Lopez-Gallego, T. R. Hoye and C. Schmidt-Dannert, *J. Bacteriol.*, 2008, **190**, 6084.

[36] A. Schifrin, Y. Khatri, P. Kirsch, V. Thiel, S. Schulz and R. Bernhardt, *Org. Biomol. Chem.*, 2016, **14**, 3385.
[37] Y. Yamada, T. Kuzuyama, M. Komatsu, K. Shin-ya, S. Omura, D. E. Cane and H. Ikeda, *Proc. Natl. Acad. Sci. U. S. A.*, 2015, **112**, 857.
[38] P. Rabe, K. A. K. Pahirulzaman and J. S. Dickschat, *Angew. Chem. Int. Ed.*, 2015, **54**, 6041.
[39] J. Rinkel and J. S. Dickschat, *Beilstein J. Org. Chem.*, 2019, **15**, 789.
[40] J. Rinkel and J. S. Dickschat, *Beilstein J. Org. Chem.*, 2019, **15**, 1008.
[41] L. Lauterbach and J. S. Dickschat, *Org. Biomol. Chem.*, 2020, **18**, 4547.
[42] J. Rinkel and J. S. Dickschat, *ChemBioChem*, 2020, **21**, 807.
[43] J. S. Dickschat, J. Rinkel, P. Rabe, A. Beyraghdar Kashkooli and H. J. Bouwmeester, *Beilstein J. Org. Chem.*, 2017, **13**, 1770.
[44] G. Li, Y.-W. Guo and J. S. Dickschat, *Angew. Chem. Int. Ed.*, 2020, **59**, accepted.
[45] J. Rinkel, S. T. Steiner and J. S. Dickschat, *Angew. Chem. Int. Ed.*, 2019, **58**, 9230.
[46] J. Rinkel, L. Lauterbach, P. Rabe and J. S. Dickschat, *Angew. Chem. Int. Ed.*, 2018, **57**, 3238.
[47] L. Lauterbach, B. Goldfuss and J. S. Dickschat, *Angew. Chem. Int. Ed.*, 2020, **59**, 11943.
[48] J. Rinkel, L. Lauterbach and J. S. Dickschat, *Angew. Chem. Int. Ed.*, 2017, **56**, 16385.
[49] J. Rinkel, L. Lauterbach and J. S. Dickschat, *Angew. Chem. Int. Ed.*, 2019, **58**, 452.
[50] Z. Li, Y. Jiang, X. Zhang, Y. Chang, S. Li, X. Zhang, S. Zheng, C. Geng, P. Men, L. Ma, Y. Yang, Z. Gao, Y.-J. Tang and S. Li, *ACS Catal.*, 2020, **10**, 5846.
[51] A. Meguro, T. Tomita, M. Nishiyama and T. Kuzuyama, *ChemBioChem*, 2013, **14**, 316.
[52] A. Hou and J. S. Dickschat, *Angew. Chem. Int. Ed.*, 2020, **59**, 19961.